Scanning Microscopy

Volume 1995
Number 9 *Luminescence*

Article 12

1995

Plagioclase Studies by Ionoluminescence (IL) and Particle-Induced X-Ray Emission (PIXE) Employing a Nuclear Microprobe

N. P. -O. Homman
University of Lund, Sweden

C. Yang
National University of Singapore

K. G. Malmqvist
University of Lund, Sweden

K. Hanghöj
Geological Museum, Öster Voldgade, Denmark

Scanning Microscopy Supplement 9, 1995 (Pages 157-165) 0892-953X/95$5.00+.25
Scanning Microscopy International, Chicago (AMF O'Hare), IL 60666 USA

PLAGIOCLASE STUDIES BY IONOLUMINESCENCE (IL) AND PARTICLE-INDUCED X-RAY EMISSION (PIXE) EMPLOYING A NUCLEAR MICROPROBE

N.P.-O. Homman, C. Yang[2], K.G. Malmqvist* and K. Hanghõj[1]

Dept. Nuclear Physics, Univ. of Lund and Lund Inst. of Technol., Sölvegatan 14, S-223 62 Lund, Sweden
[1]Geological Museum, Öster Voldgade 10, 1350 Copenhagen K, Denmark
[2]Current address: Dept. of Physics, National University of Singapore, Singapore 119260

Abstract

When an ion beam in the energy range of a few MeV/amu impacts on a mineral, visible light can often be observed. This light, termed ionoluminescence (IL), has been shown to be a very useful tool for investigating geological specimens when it is combined in a nuclear microprobe with a well-established, quantitative, trace element method such as Particle Induced X-ray Emission (PIXE). When plagioclases from the Skaergaard intrusion, East Greenland, were irradiated with protons, bluish luminescence was observed. Spectroscopic IL studies were undertaken with 1.5 and 2.5 MeV protons with power densities ranging from about 6 to 160 W/cm^2. In the IL spectra of the plagioclase specimens, four emission bands were observed, peaking at about 4200, 4600, 5500, and 7500 Å, respectively. The relative intensities of the emission bands in the short wavelength region were rather constant for all samples, except for the long wavelength band, activated by Fe^{3+} and peaking at 7500 Å, which varied considerably. Variation in the oxidation states of the samples was investigated by measuring the Fe^{3+} intensity from IL normalized to the total iron concentration as obtained by PIXE. The relationship between the Fe^{3+}-activated peak area normalized to the total iron content and the expected relative oxidation state was found to be relevant.

Key Words: IL, CL, PIXE, nuclear microprobe, beam damage, oxidation state, Fe^{3+}, plagioclase, orthoclase, albite.

*Address for correspondence:
K.G. Malmqvist, address as above.
Telephone Number: + 46 + 46 222 7741
FAX Number: + 46 + 46 222 4709

Introduction

Cathodoluminescence (CL) is a very useful tool and is a complement to the arsenal of methods for analysing geological specimens in the electron microprobe [15, 18]. The nuclear microprobe [27, 28], which utilizes focussed heavy ion beams, shows close resemblance to the electron microprobe in terms of principles and methods for analysis. Since both instruments employ charged particle beams, the luminescence phenomena produced can be expected to show similarities. Therefore, much of the experience that has been gained in CL work with various geological specimens can be of use in ionoluminescence (IL) research as well. The potential of the IL technique as a tool for the nuclear microprobe has been demonstrated recently [29, 30, 31].

The luminescence from a mineral can be enhanced by either impurity elements or different types of intrinsic defects such as nonstoichiometry, radiation damage, etc. Several of the impurity elements of interest in luminescence studies, such as rare earth elements and transition-metal elements, are of low abundance in natural minerals, frequently being found at a ppm level, although still high enough in concentration to affect the emission of luminescence from a specimen. Depending on the influence it has on the IL spectrum, an element, or rather an element in a particular chemical valence state, is denoted as being an activator, a coactivator or a quencher [15]. An activator determines the emission spectrum, whereas a coactivator is essential for emission but has no effect on the spectrum. A quencher introduces new energy levels in the band gap, resulting in either non-radiative conversion or long-wavelength infrared (IR) radiation.

The electron transitions that cause luminescence in transition metal ions and in divalent rare earth ions are more sensitive to the surrounding chemical environment than the trivalent rare earth ions, in which the electron transitions are shielded by the outer electrons $5s^25p^6$. In the former case, the luminescence peaks are expected to be broader and to show a more variable peak centre, whereas in the latter case, the luminescence peaks should be narrower and more characteristic of the ions.

In work with CL, one notes that the task of deter-

mining the correlation between CL and the trace element content of a specimen can be difficult. When employing EDX (Energy Dispersive X-ray analysis), it is difficult to obtain detection limits below the per mille level. If some other instrumental method is used for the trace element analysis, uncertainty in localizing the spatial structure in the specimen involved introduces problems in correlating results from the respective methods.

In the nuclear microprobe, these problems can be reduced considerably through the simultaneous combination of IL and a sensitive multi-element method such as PIXE (Particle Induced X-ray Emission) [10]. PIXE, combined with a nuclear microprobe, can often achieve detection limits of a few ppm and a lateral resolution of a few micrometres.

In this paper, the simultaneous use of IL and PIXE in a nuclear microprobe for the investigation of natural plagioclase minerals from the Skaergaard intrusion, East Greenland is described.

Luminescence Observations in Feldspars

The feldspars owe their importance to the fact that they are the most abundant of all minerals in the earth's crust. All of them are closely related in form and physical properties, but they fall into two subgroups: the potassium and barium feldspars, on the one hand, which are monoclinic (i.e., orthoclase), and the sodium and calcium feldspars (i.e., the plagioclases, ranging from albite to anorthite), which are triclinic. Several types of ions have been identified as luminescence activators, but not as of yet as quenchers. Currently identified transition-metal ion activators are Fe^{3+} at 7000-7800 Å [7, 14], Mn^{2+} at about 5700 Å [6, 14], and Cu^{2+} at 4200 Å [14]. The Fe^{3+} ions probably occupy Al^{3+} sites [5, 8, 17, 24], and Mn^{2+} mainly Ca^{2+} sites and sometimes Al^{3+} sites [8, 25]. Also Fe^{2+}, which is a well-known quencher in most other minerals, has shown indications in CL experiments of being an activator [14],with an emission band at 5500 Å.

Emission bands have sometimes been observed at 4075 Å and 4950 Å as well [21]. The origin of a peak observed at about 4500 Å has been discussed, some workers attributing it to lattice defects [6, 7, 8], and others considering it to be caused by Ti^{4+} [13]. It cannot be intrinsic, however, since authigenic feldspars are either non-luminescent or show very weak luminescence [11].

The question of whether Ti^{4+} is an activator or a coactivator is still being discussed, although an emission band peaking at about 4600 Å was observed when a synthetic labradorite crystal was doped with Ti^{4+} ions [14]. There is also some evidence that at high concentrations, Ga ions can serve as a luminescence activator. It is not clear how the Ga ions interact, but an emission band peaking at about 4900 Å has been observed [2]. As expected , the rare earth elements have been shown to be activators when synthetic plagioclases are doped with these elements [13, 14]. However, these elements are very rare in natural feldspars.

It has been observed that the luminescence from several kinds of plagioclases is polarized [21, 22]. On the basis of measurements and the application of ligand-field theory for Fe^{3+}, it has been suggested that emission from Fe^{3+} or Mn^{2+}, when occupying sites of a distorted tetrahedral type (generally Al^{3+} sites), is polarized [25], assuming that the site symmetry is not altered by the substitution.

Experimental Method

The experiments reported here were undertaken at the Lund Nuclear Microprobe facility [12] using a proton beam with an energy of 1.5 or 2.5 MeV. The particle- induced X-ray emission was recorded with a 50 mm^2 Si(Li) detector having an energy resolution of less than 155 eV full-width at half maximum (FWHM) at 5.9 keV. To reduce the count rate from major elements, the X-rays from the Skaergaard plagioclases were filtered through 775 μm of Mylar before entering the Si(Li) detector. The elemental concentrations were computed by the GEOPIXE evaluation code [19, 20].

The IL light collection system consists of a condenser lens, with a solid angle of 1.8 sr, mounted inside the analysing chamber close to target, another thin lens serving as a vacuum-sealing window, and still another lens focusing the light onto the entrance slits of the monochromator. All the lenses are of Optical Crown Glass™ (Melles Griot Inc., Irvine, CA). With this system, the lenses define the short wavelength cut-off at 3500 Å. More recently, a new light collection system with quartz lenses has been installed. This extends the short wavelength cut-off into the near UV, 1600 Å, set here by the sensitive range of the photomultiplier tube (PMT). In the present study, however, the old light collection system was employed. Before starting the IL investigations, the possible offset in the scanning grating system and the alignment of the lens system and of the monochromator were checked by a He-Ne laser.

The monochromator has a wavelength-dispersing distance of about half a meter and is equipped with a grating of 1200 lines/mm and a blaze wavelength of 5000 Å. For the experiments, the scanning speed of the monochromator was set to 5 or 10 Å/s, the entrance and exit slits being typically set to 800 or 2000 μm, which implies a wavelength resolution of about 16 and 40 Å, respectively.

The PMT Hamamatsu (R943-02) (Hamamatsu,

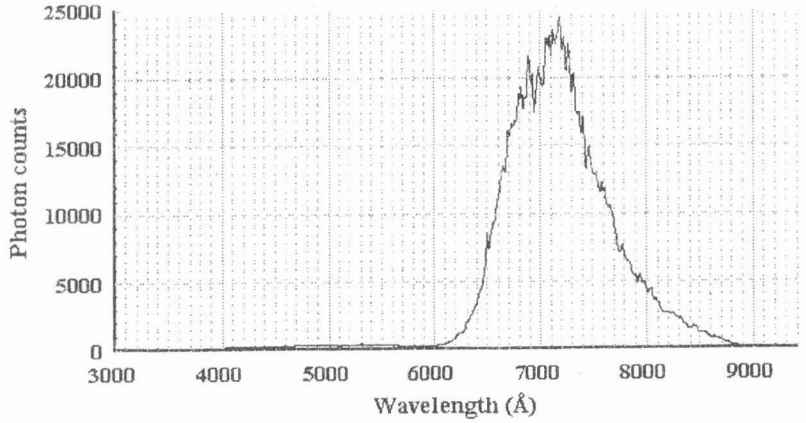

Figure 1. The IL spectrum of a Fe^{3+}-activated orthoclase X-ray standard. Beam conditions: 3.5 nA beam current, 100 x 100 μm^2 beam size, 2.5 MeV proton energy. Iron (total Fe) concentration 1.51 wt%. Monochromator settings: bandwidth 8 Å, scan speed 5 Å/s. The IL colour observed is red. The spectrum is not corrected for system efficiency.

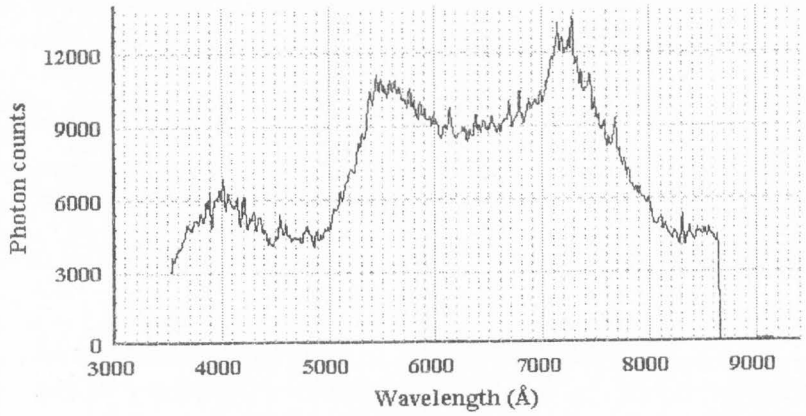

Figure 2. The IL spectrum of an albite X-ray standard. The peak at 7200 Å can probably be attributed to Fe^{3+}-activation. The emission band at 5500 Å may be due to either Mn^{2+} or Fe^{2+} activation. The IL colour observed is yellow. Beam conditions: 2.8 nA beam current, 100 x 100 μm^2 beam size, 2.5 MeV proton energy. Iron (total Fe) concentration 42 ppm, manganese concentration 4 ppm. Monochromator settings: bandwidth 16 Å, scan speed 5 Å/s. The spectrum is not corrected for system efficiency.

Shizuoka-ken, Japan) has a wavelength-sensitive region ranging from 1600 to 9400 Å. The PMT is connected directly with the exit slits of the monochromator. It is operated in single photon counting mode. To bring the dark current down, it is usually cooled to about -30°C. A typical dark current is one of 40 cps, partially defined by the stray light entering the IL system. The output signal from the PMT is amplified and is discriminated from noise. The logical output of the discriminator is then passed into a multi-channel scaling device (MCS) on a ND9900 data acquisition system for registration. Simultaneously, the proton current and back-scattered protons are acquired on other ports of the MCS, enabling corrections to be made for variations in current. It is also possible to have a second PMT, operated in panchromatic mode, connected for beam-damage and current-variation correction of the IL spectrum. The PIXE data is acquired simultaneously in the same acquisition system on an analog-to-digital converter (ADC).

Prior to nuclear microprobe analysis, the specimens were studied with an optical microscope so as to select homogenous, inclusion free regions inside the plagioclase grains for analysis. Electron microprobe analysis of the major and minor elements was also carried out prior to PIXE and IL analysis.

It should be noted that the spectra presented here have neither been corrected for instrumental response nor for beam damage. All of them were acquired at room temperature.

Results and Discussion

Standard material

In orthoclases, iron has been reported to occur mainly in the ferric state, Fe^{3+}, as determined by optical absorption spectroscopy [5]. In Figure 1, an IL emission spectrum from an orthoclase standard for X-ray analysis, MAD-10 (Charles M. Taylor Co., Stanford, CA), is presented. During proton bombardment, a reddish luminescence was observed and in the spectrum only a strong and broad emission band at about 7100 Å could be distinguished. This is in agreement with other CL observations of Fe^{3+} in orthoclase [15]. The concentration of iron in this particular specimen was 1.31 by weight (wt%), some additional trace elements

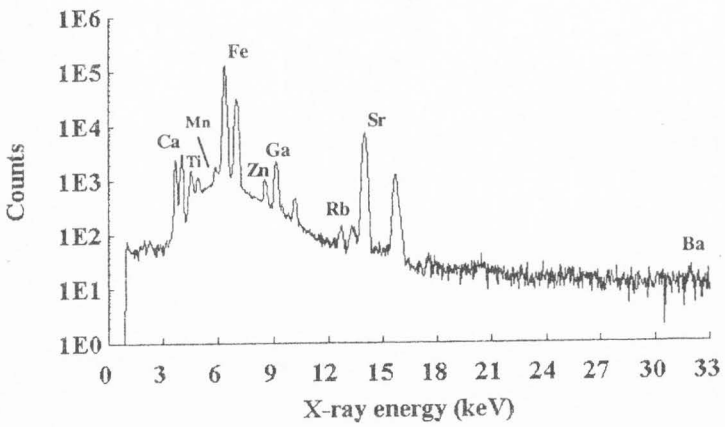

Figure 3. A typical PIXE spectrum from the plagioclase in sample no. 472 from the Skaergaard intrusion. The Si(Li) detector was equipped with a filter of 775 μm Mylar. Conditions for analysis: 2.5 MeV protons, 5 μC integrated charge, count rate 1470 cps.

found being presented in Table 1.

Figure 2 shows an emission spectrum from an albite standard, AMELIA (Charles M. Taylor Co). The PIXE analysis showed a content of 42 ppm Fe and 4 ppm Mn, some additional elements present being shown in Table 1. Even though the concentrations of the elements are very low, it is tempting to try to relate some of the emission bands to activators. The peak at 7200 Å can probably be ascribed to Fe^{3+} activation. A plausible activator for the peak at 5500 Å is Mn^{2+}, but according to Mariano *et al.* [14, 15], this wavelength can also be due to Fe^{2+}.

Natural plagioclases

The natural plagioclases analysed in the present study are from the Skaergaard intrusion, East Greenland. The rocks of the Skaergaard intrusion are predominantly gabbroic cumulates with compositions that differ from those of their parental liquids, and with mineral compositions that are modified to a varying extent by late magmatic and subsulidus processes. The samples are from the lower part of the Triple Group in the Middle Zone and constitute a depth profile of 80 metres across a gold bearing zone [1, 9]. All the plagioclase grains analysed are andesines with anorthite contents ranging from 30 to 50 mole percent and orthoclase components of less than 3 mole percent. The trace element contents are similar in all the plagioclase grains analysed. A typical PIXE spectrum from the plagioclase sample no. 472, a spectrum induced by 2.5 MeV protons, is shown in Figure 3. In total, 12 specimens from different depths were investigated and on each section one or two grains were analysed. Trace element concentrations for four of the specimens investigated are presented in Table 1.

In Figure 4, IL spectra from two specimens, no. 445-3 and no. 453-5 are shown. The broad emission band peaking at 7500 Å can be attributed to Fe^{3+}. In the short wavelength region, three broad emission bands can be identified, peaking at 4200, 4600, and 5600 Å, respectively. The wavelengths for two of the emission bands, peaking at 4600 Å and 5600 Å, seem to agree with the wavelengths observed for Ti^{4+}- and Mn^{2+}- activation in CL work [6, 14]. Whether what seems the slightly higher IL yield of manganese for sample no. 453-5 is due to a higher manganese concentration in that sample or to some other cause is difficult to infer. Whether the presence of titanium is reflected by the 4600 Å band is not clear. The occurrence of a peak at 4600 Å does seem to reflect the presence of titanium, however, since the albite spectrum shows no peak at 4600 Å and according to the PIXE analysis it has a titanium concentration of less than 5 ppm. Also, the origin of the emission band at 4200-4300 Å is unknown, but it has been observed at about the same relative intensity compared with the other emission bands in the bluish region of every spectrum, except in one grain in one of the samples, in which the relative intensity was reduced to about half. The trace element content of the latter, however, did not reveal any appreciably differing composition. A striking resemblance with the emission bands at 4200 and 4600 Å has also been observed in another silicate mineral, quartz, when cooled to about 150K. An emission band peaking at about 4000 Å can also be observed in the albite spectrum (Fig. 2).

A large difference in Fe^{3+} intensity between the two plagioclase spectra in Figure 4 can be noted. The difference is slightly less when the intensity is normalised to the iron concentration, but the difference is still considerable. The texture and mineral chemistry of sample 453-5 suggests this sample to be an orthocumulate with significant amounts of trapped interstitial liquid, and that there has been considerable reaction between the cumulus minerals and the interstitial liquid. The efficient trapping of interstitial liquid has caused a relative enrichment of volatiles dissolved in the melt,

Table 1. Trace element concentrations for four representative plagioclase specimens from the Skaergaard intrusion, and for one orthoclase- and one albite-standard. For each element, the upper number indicates the concentration and the lower the uncertainty (1σ), except for Fe^{3+}, for which two measurements are given. The PIXE data were acquired at 2.5 MeV and the Fe^{3+} data at 1.5 MeV.

	Standards		Plagioclases			
Sample / Element	Ortho-clase	Albite	445-3	453-5	462	472
Ti (ppm)	-	<5	570 25	582 27	553 24	641 26
Mn (ppm)	-	3.8 1.6	17 1.3	28 1.2	35 1.2	21 1
Fe (%w)	1.51 0.24	42 3.7	0.315 0.005	0.496 0.009	0.354 0.005	0.338 0.005
Zn (ppm)	25 2.2	12 0.7	15 0.5	15 0.7	13 0.5	12 0.4
Ga (ppm)	58 4	72 2	44 0.8	48 1.3	40 0.8	43 1.4
Rb (ppm)	742 16	-	<1.78	2.85 1.4	4.3 1.0	3.5 0.7
Sr (ppm)	14 1.2	24 1.5	689 9	787 14	658 12	652 11
Ba (ppm)	737 56	-	209 39	139 46	180 35	209 54
Fe^{3+} (cps)	-	-	463 425	1540 999	364 424	579 566
Fe^{3+}/Fe (cps/ %w)	-	-	1470 1350	3100 2010	1030 1200	1710 1670

thus yielding a relatively high oxygen fugacity. Sample 445-3 can be characterized as an accumulate with little or no entrapment of interstitial liquid, volatiles having thus been able to escape to higher levels. Sample 453-5, therefore, can be expected to have a higher Fe^{3+}/Fe^{2+} ratio than sample 445-3. The possibility of employing this for oxidation state measurements will be discussed below.

The samples were all prepared as ordinary carbon-coated thin polished sections with a thickness of about 30 μm (8 mg/cm^2). Since a proton beam with an energy of 2.0 MeV or higher penetrates this thickness, the glass substrate was also analysed under the same conditions as the plagioclases. The IL emission from the glass substrate was very weak, however, and showed only a broad emission band at 5000 Å. The IL spectra presented in Figure 4 were produced using 2.5 MeV protons. The thickness variation between different samples was estimated to be less than 15 percent. The generally slightly higher luminescence yields for sample 453-5 can thus also be partially due to a slightly thicker sample.

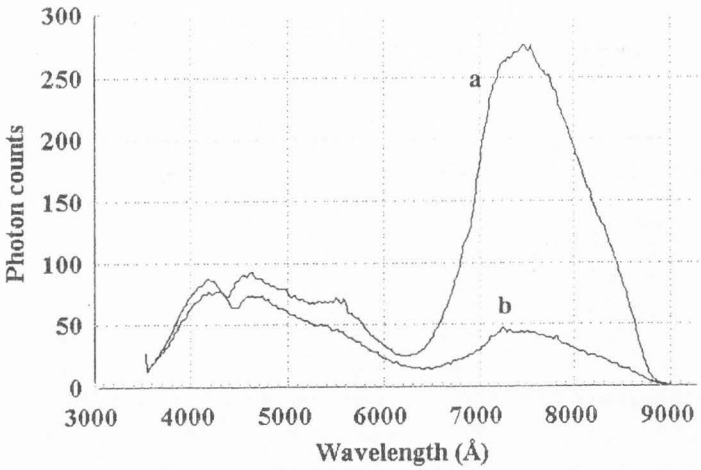

Figure 4. IL spectra of plagioclases from two thin sections, samples no. 453-5 (A) and no. 445-3 (B), from the gold bearing zone of the Skaergaard intrusion, East Greenland. The variation in the Fe^{3+} peak at 7500 Å is notable. The 453-5 sample is expected on the basis of textural and geochemical investigation to show a higher Fe^{3+}/Fe^{2+} ratio. The iron (total Fe) concentration is 0.315 and 0.496 wt% for samples 445-3 and 453-5, respectively. The IL colour observed is blue. Beam conditions: 3.5 nA beam current, 100 x 100 μm^2 beam size, 2.5 MeV proton energy. The spectra are not corrected for system efficiency. Monochromator settings: bandwidth 16 Å, scan speed 10 Å/s.

Comparison of IL yields is apparently more difficult when specimens are not infinitely thick. The reason for maintaining high proton energy is partly that the PIXE sensitivity of heavier elements decreases considerably at lower proton energies and partly to reduce the energy deposition per micrometre in the sample (the energy loss per micrometre is higher at reduced proton velocity) while maintaining the proton current.

Oxidation state measurements

A means of extracting information concerning the Fe^{3+}/Fe^{2+} ratio from the luminescence spectra of feldspars has been suggested by Mariano *et al.* [14], who proposed to employ the CL intensity for the Fe^{3+} and the Fe^{2+} emission bands. However, the Fe^{2+} emission band, 5500 Å, usually overlaps with other broad emission bands in the same region, such as that of Mn^{2+}. This can make the determination task rather difficult. Even without the Fe^{2+} peak, it should be possible, however, to extract similar information if the Fe^{3+} luminescence intensity is related to the total iron concentration in the specimen. This assumes that iron is present only as Fe^{2+} and Fe^{3+}. This is held to be true in terrestrial geological samples. Any approach that utilizes luminescence implies that the Fe^{3+} or Fe^{2+} activated lumines-

cence is not quenched by other elements and that the luminescence yields as a function of iron content are known. According to Telfer *et al.* [25], Mn^{2+} and Fe^{3+} yields respond linearly to the total content of the element for concentrations up to 0.5 mole percent, the yield above this concentration approaching saturation.

To avoid problems connected with the proton penetration of the samples, the proton energy was lowered to 1.5 MeV for investigating the oxidation state. In previous wavelength dispersive IL investigations of such specimens, it was observed that the Fe^{3+} emission band was very broad and that it peaked at 7500 Å in all specimens. Therefore, the monochromator was set at 7500 Å, with a bandwidth of 40 Å. The beam current was 0.1 nA in a 20 x 120 μm^2 beam spot and the current density 0.04 pA/μm^2. Four specimens were selected for investigation of the oxidation state. Two of them, samples 453-5 and 472, were expected in terms of their textural and geochemical signatures to show a higher Fe^{3+}/Fe^{2+} ratio. Two grains were analysed in each thin section. Since the decay rate of the luminescence yield as a function of proton irradiation time was roughly constant for all the samples investigated, the yield was integrated in the interval 250-350 seconds after the start of irradiation.

In Table 1, the Fe^{3+} yields normalised to the iron concentration are presented for the plagioclase specimens. The IL results in the table appear to be in accordance with geochemical evidence of a higher oxidation state obtained for samples 453-5 and 472. These data also agreed with the wavelength dispersive IL data previously acquired at 2.5 MeV. A comparison of the Fe^{3+} yields and the iron concentrations for all the IL spectra (12 specimens) indicates that the method for relative oxidation state measurements presented to be applicable. Although a relationship was found between the IL/PIXE and the expected Fe^{3+}/Fe^{2+} ratio, this cannot be taken as proof that the relationship is genuine before a more comprehensive investigation of effects of the presence of other elements on the Fe^{3+} yield has been carried out. To make the method quantitative, if at all possible, some standard material of feldspars with well-characterized Fe^{3+}/Fe^{2+} ratios is required. Further IL investigation of this material will be undertaken and will be compared with the results of Mössbauer spectroscopy.

Beam damage

Several workers have employed proton beams for the luminescence investigation of feldspars [3, 4, 6, 16], all with power densities in the order of mW/cm^2, however. Derham *et al.* [3] varied the proton energy from 5 to 100 keV without registering any change in the IL spectral shape. They also investigated 2 and 4 MeV protons with the same result. For single mineral grain studies, the dimensions of the grain often requires that the probe have a dimension of only a few micrometres. If the beam current is to be maintained, this can easily result in power densities in the order of kW/cm^2 in a nuclear microprobe at ordinary settings with a voltage of 2.5 MV, a beam current of 1 nA and a beam spot diameter of 10 μm. During the bombardment of a specimen with heavy ions, several different processes such as sample heating, sputtering, proton implantation and track effects take place in the specimen [26]. This inevitably affects the IL yield. At the high power density here, the PIXE analysis of geological specimens is a minor problem, even though sample heating must also be considered. In the current experimental setup, a few nA of protons are required for wavelength dispersive IL, just as they are for the trace element analysis by PIXE of most minerals such as apatites, titanites, zircons and feldspars. Therefore, if no zonation of the mineral grains is observed or expected, as broad a beam as possible is employed for IL analysis.

In Figure 5, two consecutive IL spectra from the same location but with a 4 μC proton bombardment interval are presented. The proton energy was 2.5 MeV and the beam current 3.5 nA in a 100 x 100 μm^2 beam spot. During the acquisition of a spectrum, the sample was irradiated with another 2 μC. The reduction in the IL yield for short wavelengths appears to be more severe than for longer wavelengths, but this is mainly an effect of the manner of acquiring the data. Since the monochromator is scanned from short towards longer wavelengths with a scanning speed of 10 Å/s, a considerable number of protons have already bombarded the specimen when the Fe^{3+} peak is approached. It can be noted that the relative change in the bluish region is similar for all the emission bands. In investigating proton energy dependence, IL spectra were obtained at three different proton energies: 1.5, 2.0 and 2.5 MeV. No relative changes in spectrum shape were observed, except for a generally lower IL yield at lower proton energies.

As long as the beam damage is similar for all the wavelengths, a second PMT, operated in panchromatic mode, can be employed for correcting the data. Before adopting this approach, one should investigate the IL yield response to proton bombardment of all the features of interest in the spectrum. The time dependence can also be of interest since IL records changes in the defect state of the sample during bombardment and can thus provide information on the growth or decay of intrinsic defects, as well as on pre-existing imperfections [25]. The IL yield decay rate in one plagioclase specimen was investigated for three wavelengths, 4650, 5650, and 7500 Å, using 2.5 MeV protons, at 66 μA/cm^2 current density for the latter wavelength and at 35 μA/cm^2 for

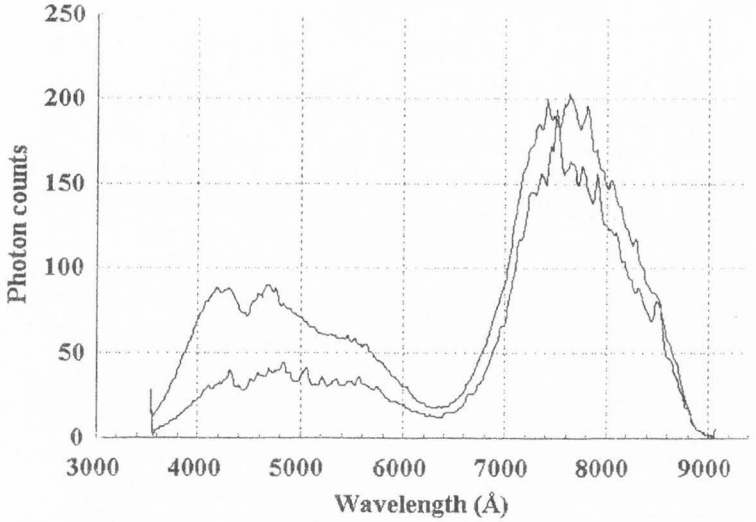

Figure 5. Consecutive IL spectra from plagioclase sample no. 453-5, separated through 22 minutes of 3.5 nA proton bombardment in a 100 x 50 μm^2 beam spot. The decay of the Fe^{3+} appears to be less than for short wavelengths but this is the effect of the spectrum being acquired from short to long wavelengths at a scan speed of 10 Å/s. Monochromator setting: bandwidth 16 Å.

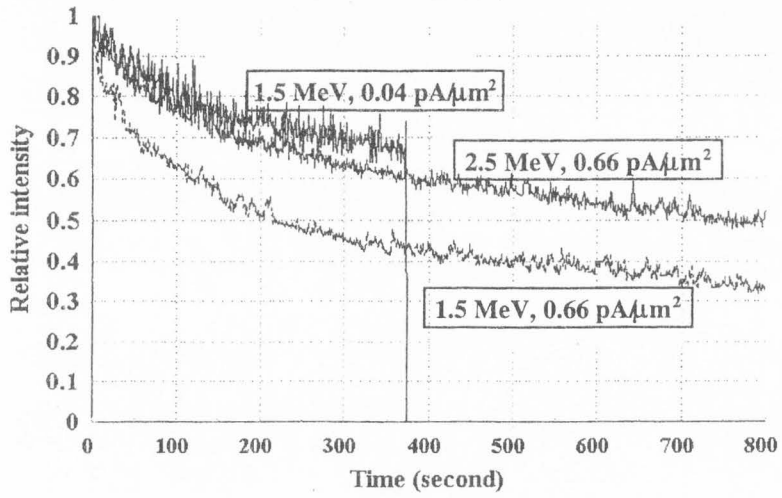

Figure 6. IL yield decay at 7500 Å (Fe^{3+}) in a plagioclase as induced by 1.5 MeV or 2.5 MeV protons. In comparing the different proton energies, note that the 2.5 MeV protons penetrate the sample thickness, depositing only 1 MeV in the sample.

the two former ones. The decay rate was found to be similar for all wavelengths, there being a reduction of 2-2.5 times after 800 seconds of bombardment. Generally, short wavelengths suffer more from an introduction of new energy levels than long wavelengths.

The Fe^{3+} yield was also studied at two different current densities, 4 and 66 $\mu A/cm^2$, and at two different proton energies, 1.5 and 2.5 MeV, as shown in Figure 6. To obtain beam damage conditions as comparable as possible, a fresh location on the sample was chosen for the 100 x 100 μm^2 beam at every irradiation. The monochromator was set at 7500 Å with a bandwidth of 40 Å, the Fe^{3+} yield being monitored as a function of irradiation time with a dwell time of 1 second. From the figure, it is apparent that a higher current density introduces damage to the sample much earlier. For a constant proton charge, a difference of a factor of about ten in the short term decay rate can be noted for 1.5 MeV protons. This is of about the same order of magnitude as the difference in current density.

Comparing 1.5 and 2.5 MeV, one can probably attribute the more rapid decay with the lower energy to a higher energy deposition per micrometre of penetration for the 1.5 MeV protons. It can be noted that the 2.5 MeV protons deposit about 1 MeV in their passage through the plagioclase specimen (30 μm), which on the average is 33 keV/μm. The 1.5 MeV beam deposits its energy at about 23 μm, which on the average is 64 keV/μm. For ions of low mass, such as protons, the energy loss through electronic excitation (dE/dx) dominates at high energies, whereas nuclear collisions are of importance only at the very end of the range, where the speed of the ion is reduced. Thus, in the case of 2.5 MeV protons, the interaction in the plagioclase is almost exclusively electronic, whereas in the case of 1.5 MeV, it is also to a minor part nuclear, which can lead to displacement of the lattice ions and to secondary collisions. Also, for electron beams, a decay in the Fe^{3+} yield has been observed. Geake *et al.* [8] attributed this decay, at least in part, to the reducing effect of the electron beam converting Fe^{3+} to Fe^{2+}.

By replacing the PMT with a solid state array detec-

tor, the beam damage problems can be reduced considerably. Such a detector is capable of registering the complete spectrum simultaneously. Its potential usefulness in research on beam damage processes seems, therefore, considerable.

Conclusions

The possibility of simultaneously measuring Ionoluminescence (IL) and the trace element content in a nuclear microprobe by use of PIXE has been shown to represent a very promising tool in the search for luminescence activators and quenchers in minerals. However, in using heavy-ion beams in IL investigations, beam damage must be taken into account, especially when a scanning monochromator system is employed.

The possibility of measuring the relative oxidation state in plagioclases by means of the Fe^{3+}/Fe^{2+} ratio in plagioclases was investigated through employing intensity information from IL concerning Fe^{3+} and from PIXE concerning the total iron content. The results were generally in agreement with the expected relative oxidation states based on geochemical evidence for oxygen fugacities. However, further investigation is needed to learn more about the method and develop it as a quantitative tool.

Acknowledgement

The authors would like to thank the Swedish Natural Research Council and the Royal Physiographic Society in Lund for financial support.

References

[1] Bird DK, Brooks CK, Gannicott RA, Turner PA (1991) A gold-bearing horizon in the Skaergaard intrusion, East Greenland. Econ Geol **86**: 1083-1092.

[2] de St. Jorre L, Smith DGW (1988) Cathodoluminescent gallium-enriched feldspars from the Thor lake rare-metal deposits, Northwest territories. Can Mineral **26**: 301-308.

[3] Derham CJ, Geake JE, Walker G (1964) Luminescence of enstatite achondrite meteorites. Nature **203**: 134-136.

[4] Edgington JA, Blair JA (1970) Luminescence and thermoluminescence induced by bombardment with protons of 159 million electron volts. Science **167**: 715-717.

[5] Faye GH (1969) The optical absorption spectrum of tetrahedrally bonded Fe^{3+} in orthoclase. Can Mineral **10**: 112-117.

[6] Geake JE, Walker G, Mills AA, Garlick GFJ (1971) Luminescence of Apollo lunar samples. Proc Second Lunar Conf 3. Geochim Cosmochim Acta, Suppl 2: 2265-2275.

[7] Geake JE, Walker G, Telfer DJ, Mills AA, Garlick GFJ (1973) Luminescence of lunar, terrestrial, and synthesized plagioclase, caused by Mn^{2+} and Fe^{3+}. Proc Fourth Lunar Conf 3. Geochim Cosmochim Acta, suppl 4: 3181-3189.

[8] Geake JE, Walker G, Telfer DJ, Mills AA (1977) The cause and significance of luminescence in lunar plagioclase, Phil Trans Royal Soc Lond A **285**: 403-408.

[9] Hanghöj K (1993) Petrographic description of the Au-PGE mineralization in the Skaergaard intrusion: Evidence for the evolution of the Skaergaard liquid. Cand scient thesis, University of Copenhagen.

[10] Johansson SAE, Campbell JL. (1988) PIXE: A Novel Technique for Elemental Analysis. Wiley, Chichester, U.K., pp. 1-40.

[11] Kastner M (1971) Authigenic feldspars in carbonate rocks. Am Mineral **56**: 1403-1442.

[12] Malmqvist KG, Hylten G, Hult M, Hakansson K, Knox JM, Larsson NOO, Nilsson C, Pallon J, Schofield R, Swietlicki E, Tapper USA, Yang C (1993) Dedicated accelerator and microprobe line. Nucl Instrum Meth **B77**: 3-7.

[13] Mariano AN, Ring PJ (1975) Europium-activated cathodoluminescence in minerals. Geochim Cosmochim Acta **39**: 649-660.

[14] Mariano AN, Ito J, Ring PJ (1973) Cathodoluminescence of plagioclase feldspars. Abstracts with Programs 5. Geological Society of America, Boulder, CO. p. 726 (abstract).

[15] Marshall DJ (1988) Cathodoluminescence of Geological Materials. Unwin Hyman, London, U.K., pp. 111-123.

[16] Nash DB (1973) Experimental results on combined ultraviolet-proton excitation of moon rock luminescence. J Geophys Res **78**: 3512-3514.

[17] Pott GT, McNicol BD (1972) Zero-phonon transition and fine structure in the phosphorescence of Fe^{3+} ions in ordered and disordered $LiAl_5O_8$. J Chem Phys **56**: 5246-5254.

[18] Remond G, Cesbron F, Chapoulie R, Ohnenstetter D, Roques-Carmes C, Schvoerer M (1992) Cathodoluminescence applied to the microcharacterization of mineral materials: A present status in experimentation and interpretation. Scanning Microsc **6**: 23-68.

[19] Ryan CG, Clayton E, Cousens DR, Griffin WL, Sie SH (1988) SNIP, a statistics-sensitive background treatment for the quantitative analysis of PIXE spectra in geoscience applications. Nucl Instrum Meth **B34**: 396-402.

[20] Ryan CG, Cousens DR, Griffin WL, Sie SH, Suter GF (1990) Quantitative PIXE microanalysis of

geological material using the CSIRO proton microprobe. Nucl Instrum Meth **B47**: 55-71.

[21] Sippel RF (1971) Luminescence petrography of the Apollo 12 rocks and comparative features in terrestrial rocks and meteorites. Proc Second Lunar Conf **1**. Geochim Cosmochim Acta, Suppl 2: 247-263.

[22] Smith JV, Stenstrom RC (1965) Electron-excited luminescence as a petrologic tool. J Geol **73**: 627-635.

[23] Swietlicki E, Larsson NPO, Yang C (1993) Multivariate statistical processing of elemental maps from nuclear microprobes. Nucl Instrum Meth **B77**: 195-202.

[24] Telfer DJ, Walker G (1975) Optical detection of Fe^{3+} in lunar plagioclase. Nature **258**: 694-695.

[25] Telfer DJ, Walker G (1978) Ligand field bands of Mn^{2+} and Fe^{3+} luminescence centres and their site occupancy in plagioclase feldspars. Mod Geol **6**: 199-210.

[26] Townsend PD (1987) Optical effects of ion implantation. Rep Prog Phys **50**: 501-558.

[27] Vis D (1985) The Proton Microprobe: Applications in the Biomedical Field. CRC Press, Boca Raton, FL, pp. 10-52.

[28] Watt F, Grime GW (1987) Principles and Applications of High-Energy Ion Microbeams. IOP Publishing Limited, Bristol, U.K., pp. 79-154.

[29] Yang C, Larsson NPO, Swietlicki E, Malmqvist KG, Jamieson DN, Ryan CG (1993) Imaging with ionoluminescence (IL) in a nuclear microprobe. Nucl Instrum Meth **B77**: 188-194.

[30] Yang C, Homman NP-O, Johansson L, Malmqvist KG (1994) Microcharacterizing zircon mineral grain by ionoluminescence combined with PIXE. Nucl Instrum Meth **B85**: 808-814.

[31] Yang C, Homman NPO, Malmqvist KG, Johansson L, Halden NM, Barbin V (1995) Iono;uminescence: a new tool for nuclear microprobe in geology. Scanning Microsc **9**: 43-62.